Powders & Grains 97, Behringer & Jenkins (eds) © 1997 Balkema, Rotterdam, ISBN 90 5410 884 3

Investigation of $f/2$ and $f/4$ waves in granular beds subject to vertical, sinusoidal oscillations

Carl R. Wassgren
Department of Mechanical Engineering, Clemson University, S.C., USA
Melany L. Hunt & Christopher E. Brennen
Department of Mechanical Engineering, California Institute of Technology, Pasadena, Calif., USA

ABSTRACT: When a deep bed of granular material is subject to vertical, sinusoidal oscillations, a number of phenomena appear including two regimes of standing surface waves that form at one-half and one-quarter of the oscillation forcing frequency. These waves are referred to as *f*/2 and *f*/4 waves where f is the oscillation frequency. This paper presents the results from experiments and computer simulations designed to study the wavelength and wave amplitude dependence of the surface waves on the vibration parameters, collision coefficient of restitution, and the particle bed depth.

1 INTRODUCTION

When a deep bed of granular material is subject to vertical, sinusoidal oscillations a number of phenomena appear including side wall convection cells, kinks and kink convection cells, and surface waves. The mechanisms causing some of these phenomena are not fully understood. Indeed, some fundamental measurements of the properties of these behaviors have not yet been made.

Of particular interest in this paper is the surface wave phenomenon. Standing waves appear on the free surface of the granular bed depending on the dimensionless acceleration amplitude of the forcing oscillations, $\Gamma=a\omega^2/g$ where a is the oscillation amplitude, ω is the oscillation radian frequency, and g is the acceleration due to gravity. The frequency of the wave formation depends on whether the range of Γ is greater or less than the first flight-time bifurcation value of $\Gamma_1\equiv3.6$ (refer to Wassgren *et al.*, 1996). When the range of Γ at which the waves appear is less than Γ_1 the waves form at one-half the oscillation frequency, f, and are termed *f*/2 waves. When the range of Γ over which the waves appear is greater than Γ_1 the waves form at one-quarter the oscillation frequency and are termed *f*/4 waves.

Previous experiments have investigated the wave patterns that occur when containers with cross-sectional aspect ratios near unity are used (Melo *et al.*, 1994, 1995; Metcalfe *et al.*, 1996; Clément *et al.*, 1996; Umbanhower *et al.*, 1996). These experiments have shown that wave patterns consisting of stripes, squares, pentagons, hexagons, and "oscillons" appear depending on the oscillation parameters. Additional experiments have examined the parameters governing the onset and wavelength of the waves (Melo *et al.*, 1994, 1995; Metcalfe *et al.*, 1996; Clément *et al.*, 1996; Wassgren *et al.*, 1996) as well as the wave amplitude (Wassgren *et al.*, 1996; Clément *et al.*, 1996). Recent discrete element computer simulations have also reported the appearance of standing surface waves and have been used to study the wavelength dependence on the vibration parameters and bed depth (Wassgren, 1996; Luding *et al.*, 1996). This paper presents the results of experiments and discrete element computer simulations designed to study the wavelength and wave amplitude dependence of the surface waves on the vibration parameters, collision coefficient of restitution, and the particle bed depth.

2 EXPERIMENTS

The experiments utilized a rectangular lucite cell with smooth glass interior walls (interior cross-sectional dimensions of 13.5x1.2cm) mounted on an electromagnetic vibration exciter that provided the vertical, sinusoidal oscillations. The container was

filled with 1.3mm diameter soda lime glass spheres to a uniform depth of approximately 13mm (h_0/d=10 where h_0 is the depth of the level bed and d is the particle diameter).

A video camera and strobe lamp were used to observe the motion of the surface waves and measurements of the wave amplitude and wavelength were made using a scale taped to the rear wall of the container. Preliminary experiments established that, for the frequencies examined (15<f<40 Hz), the formation of the surface waves depends on the dimensionless acceleration amplitude of the oscillations, $\Gamma=a\omega^2/g$. For example, at an oscillation frequency of 30 Hz the *f*/2 waves appear for 2.8<Γ<4.6 while the *f*/4 waves occur for Γ>5.8 to at least Γ=7.8 (the highest acceleration examined in these experiments). For 4.6<Γ<5.8, waves formed erratically and a clearly defined wave frequency and pattern could not be discerned. These ranges are similar to those found in the experiments of Melo *et al.* (1995) using beds of bronze spheres.

Measurements of the standing wave wavelength, λ, defined as the distance between neighboring wave peaks, were made for the *f*/4 waves. Measurements were attempted for the *f*/2 waves but the data was widely scattered due to the uncertainty in determining the lateral position of the observed rounded wave peaks. The *f*/4 waves, however, exhibit a cusp-shaped wave and the location of the wave peaks is more accurately determined. The data for the *f*/4 waves show that the wavelength increases linearly with the square of the inverse oscillation frequency, $1/f^2$ (refer to figure 1) - a dispersion relation similar to that found for deep water gravity waves. A similar trend has been observed for *f*/2 waves in experiments by Melo *et al.* (1994), Metcalfe *et al.* (1996), and Clément *et al.* (1996). Furthermore, the wavelength increases with increasing oscillation amplitude and velocity amplitude over the range of f and Γ examined. This observation is in contrast to that reported by Clément *et al.* (1996) who found that λ remains constant with Γ for a fixed frequency. The present observation, however, is in agreement with the observations by Metcalfe *et al.* (1996) (at low frequencies) and Melo *et al.* (1994). Note that the observations reported by all of these investigators were made for *f*/2 waves.

Measurements were also made of the maximum wave amplitude, η, defined as one-half the maximum elevation difference from a trough to a neighboring peak. As shown in figure 2 the maximum amplitude increases linearly with the oscillation amplitude, a, for both the *f*/2 and *f*/4 waves. Note that the slope of the data for the *f*/4 waves is approximately twice that for the *f*/2 waves. Recent experiments by Clément *et al.* (1996) have shown similar trends. It is interesting to observe that the data collapses to a single curve when plotted in terms of a Froude number, $Fr=a\omega/(g\eta)^{1/2}$, as a function of the dimensionless acceleration amplitude, $\Gamma=a\omega^2/g$. For example, the Froude number increases from Fr≅1.0 at Γ=2.6 to Fr≅1.5 at Γ=4.6 for the *f*/2 waves while for the *f*/4 waves the Froude number remains at a nearly constant value of Fr≅1.3 for 6.0<Γ<7.8.

3 COMPUTER SIMULATIONS

Two-dimensional discrete element computer simulations were also conducted to determine the effects of the vibration parameters and particle properties on the standing wave amplitude and wavelength. The simulation environment consisted of a container with a rigid base oscillating with a specified amplitude, a, and frequency, f, in a vertical, sinusoidal trajectory. Periodic boundaries were used at the lateral walls in order to eliminate wall effects. The container was filled with circular particles with a uniform diameter distribution between a specified minimum and maximum. The only forces acting on the particles were a gravity body force and particle-particle and particle-floor contact forces. The contact model consisted of a damped linear spring in the normal contact direction. Note that although surface waves continue to occur when tangential contact forces are included, all of the simulations presented here used frictionless particles in order to simplify the contact model.

A few comments should be made regarding the choice of the simulation parameters. In all of the simulations the particle/particle and particle/floor coefficients of restitution, ε_{pp} and ε_{pf}, were equal. The baseline simulation used a value of $\varepsilon=\varepsilon_{pp}=\varepsilon_{pf}$ equal to 0.5. When larger values are used for ε particle saltation on the bed's free surface increases and the waves become "smeared" and difficult to discern. Lastly, all of the simulations are performed in a 300 particle diameter wide container. This width was chosen as a compromise between reducing the degree of influence of the container width on the surface wave wavelength and minimizing the number of particles in the simulation. The remainder of the baseline simulation parameters are given in table 1.

Three properties of the surface waves were measured in the simulations: the wavelength,

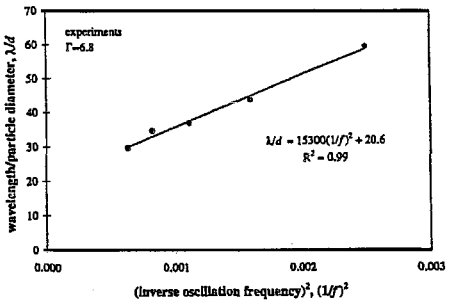

Figure 1. Wavelength plotted against the inverse frequency squared for the *f*/4 waves at Γ=6.8 (experiments).

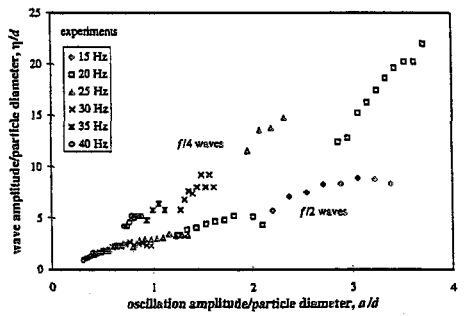

Figure 2. Maximum wave amplitude plotted against the oscillation amplitude for the *f*/2 and *f*/4 waves (experiments).

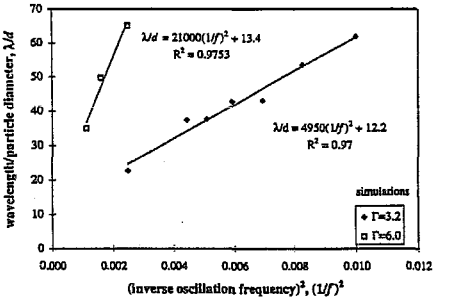

Figure 3. Wavelength plotted against the inverse frequency squared for the *f*/2 and *f*/4 waves (simulations).

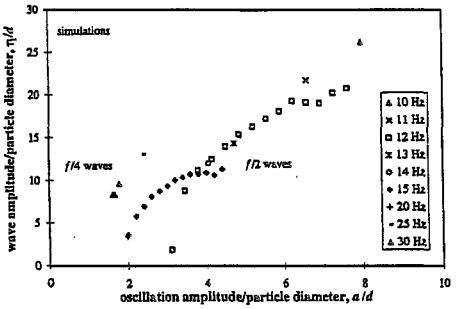

Figure 4. Maximum wave amplitude plotted against the oscillation amplitude for the *f*/2 and *f*/4 waves (simulations).

Table 1. Simulation baseline parameters.

coefficient of restitution, ε	0.5
particle/particle contact stiffness, k_{pp}	$3.6*10^3$ N/m
particle/particle contact damping, ν_{pp}	$2.1*10^{-2}$ N/(m/s)
particle/floor contact stiffness, k_{pf}	$7.2*10^3$ N/m
particle/floor contact damping, ν_{pf}	$4.2*10^{-2}$ N/(m/s)
simulation time step, Δt	$4.3*10^{-6}$ s
particle diameter, *d*	0.9 - 1.1 mm
particle density, ρ	2500 kg/m^3
number of particles, *N*	4500
dimensionless container width, *W*/*d*	300
dimensionless level bed depth, h_0/d	15
oscillation frequency, *f*	15 Hz
dimensionless oscillation acceleration amplitude, $\Gamma=a\omega^2/g$	3.2

maximum wave amplitude, and the phase angle at which the maximum wave amplitude occurred. These properties were measured as a function of the oscillation amplitude, oscillation frequency, particle bed depth, and the coefficient of restitution.

In order to measure the wave properties, the free surface profile of the bed was determined using the following procedure. The container was divided into vertical bins with a width of approximately three particle diameters. The height of the free surface above the container floor in a bin was defined as the elevation at which 95% of the total particle area in the bin was below the evaluation height. High frequency fluctuations in the surface profile data were then filtered out using an averaging window consisting of the current and the two neighboring data points. The wave amplitude and wavelength were measured from the resulting filtered surface profile data. Note that each data point for the wavelength and wave amplitude at a particular operating condition is an average value over 35 oscillation cycles.

First the wavelength dependence on the vibration parameters is discussed. In figure 3, the wavelength is plotted as a function of the inverse oscillation frequency squared. A clear linear dependence is observed with the slope of the simulated data for the *f*/2 waves being approximately one-quarter that of the *f*/4 waves. Note, however, that in the simulations the wavelength is independent of the oscillation amplitude and velocity amplitude for both the *f*/2 and *f*/4 waves.

The maximum wave amplitude and the oscillation

phase angle at which it occurs were also examined as a function of the oscillation parameters. Figure 4 shows that the maximum wave amplitude is roughly proportional to the oscillation amplitude for the *f*/2 waves (there are not enough data points for the *f*/4 waves to discern a clear trend). This relation is identical to that found experimentally. It is interesting to note that at a fixed frequency, the wave amplitude decreases rapidly for low values of the oscillation amplitude and plateaus in the upper range. These same trends can be seen in the experimental data shown in figure 2.

The phase angle at which the maximum wave amplitude occurs, ϕ, was also measured using the simulations. In all of the simulations, the maximum wave amplitude occurs just as the particle bed collides with the floor after being in-flight. The simulations indicate that ϕ increases nearly linearly with increasing Γ for the range of f and Γ examined. Furthermore, ϕ also increases with increasing frequency.

The effect of the coefficient of restitution, ε, on the wavelength and amplitude of the *f*/2 surface waves was also investigated. The wavelength of the surface waves does not vary significantly with coefficient of restitution for $0.1<\varepsilon<0.8$, although a slight increase in λ occurs with increasing ε. Higher values of ε were not investigated due to the considerable saltation on the free surface of the bed for $\varepsilon>0.8$. The wave amplitude slowly decreases with increasing coefficient of restitution for $\varepsilon<0.7$; however, at $\varepsilon\approx0.7$ the amplitude decreases significantly. The observation that the waves do not change considerably at low ε is in contrast to the conclusion by Melo *et al.* (1994) that the waves should disappear for very low values of ε.

Lastly, the effect of the particle bed depth, h_0, on the wave amplitude and wavelength was also examined for the *f*/2 waves. The wavelength increased with increasing particle bed depth and approached an asymptotic value for $h_0/d>15$, where d is the mean particle diameter. This trend is in agreement with the experimental observations by Melo *et al.* (1994) and Clément *et al.* (1996). Additionally, the amplitude decreases slowly with increasing bed depth.

4 CONCLUSIONS

The results from the simulations and experiments compare well. Both methods indicate that the wavelength of the surface waves increases linearly with the square of the inverse frequency $(1/f)^2$ and that the maximum wave amplitude increases linearly with the oscillation amplitude. Additional results from the simulations suggest that the coefficient of restitution, ε, for the particle collisions does not greatly affect the observed wavelength or amplitude except at large values of ε. Furthermore, the wavelength of the waves increases with increasing bed depth and eventually reaches an asymptotic value. The wave amplitude, however, decreases only slightly with increasing bed depth.

5 REFERENCES

Clément, E., Vanel, L., Rajchenbach, J., and Duran, J., 1996, "Pattern formation in a vibrated 2D granular layer," *Physical Review E*, Vol. 53, No. 3, pp. 2972-2975.

Luding, S., Clément, E., Rachenbach, J., and Duran, J., 1996, "Simulations of pattern formation in vibrated granular media," preprint.

Melo, F., Umbanhower, P., and Swinney, H.L., 1994, "Transition to parametric wave patterns in a vertically oscillated granular layer," *Physical Review Letters*, Vol. 72, No. 1, pp. 172-175.

Melo, F., Umbanhower, P.B., and Swinney, H.L., 1995, "Hexagons, kinks, and disorder in oscillated granular layers," *Physical Review Letters*, Vol. 75, No. 21, pp. 3838-3841.

Metcalf, T.H., Knight, J.B., and Jaeger, H.M., 1996, "Standing wave patterns in shallow beds of vibrated granular material," preprint.

Umbanhower, P.B., Melo, F., and Swinney, H.L., 1996, "Localized excitations in a vertically vibrated granular layer," *Nature*, Vol. 382, pp. 793-796.

Wassgren, C.R., Hunt, M.L., and Brennen, C.E., 1996, "Vertical vibration of a container of granular material," *Journal of Applied Mechanics*, Vol. 68, pp. 170-175.

Wassgren, C.R., 1996, *Vibration of Granular Materials*, Ph.D. Thesis, California Institute of Technology, Pasadena, CA.